Scalable 3D X-ray Computed Tomography Measurement and Accuracy for Metal Additive Manufacturing

Chaoyu Dong[1,3], Marcus Jun Qi Ng[1], Hwee Ping Ng[2], Weili Wang[2], Tong Liu[1], Andrew A. Malcolm[1]

1 Singapore Institute of Manufacturing Technology (SIMTech), Agency for Science, Technology and Research (A*STAR), 5 CleanTech Loop #01-01, CleanTech Two Block B, Singapore 636732, Republic of Singapore

2 Advanced Remanufacturing & Technology Centre (ARTC), Agency for Science, Technology and Research (A*STAR), 3 CleanTech Loop, #01-01 CleanTech Two, Singapore 637143, Republic of Singapore

3 College of Computing and Data Science, Nanyang Technological University, 50 Nanyang Avenue, Singapore 639798, Republic of Singapore

Corresponding Author / Email: dongcy@simtech.a-star.edu.sg, TEL: +65-97716329

KEYWORDS: X-ray, Computed Tomography, 3D, Precision measurement, Additive Manufacturing

In metal Additive Manufacturing (AM), component size variability presents distinct challenges for quality control and inspection, especially in X-ray Computed Tomography (XCT) measurement. Larger components typically require lower resolutions to cover their entire volume within a reasonable time frame, which can compromise the detection of smaller defects. To address this, a scalable 3D XCT measurement approach is developed in this work that maintains high resolution by stitching X-ray images in the projection domain. This proposed approach captures X-ray projection images while adjusting the component's position in an arranged grid, ensuring that the voxel size remains consistent across all projections. A linear blending strategy is then applied to smoothly manage the overlapping areas between the stitched images, resulting in an expanded coverage of the metal AM component without sacrificing detail. Finally, the Filtered Back-Projection (FBP) algorithm is used on these stitched and scaled X-ray images to generate 3D reconstructions. The performance and measurement accuracy of this scalable 3D XCT measurement are experimentally evaluated using Laser-based Powder Bed Fusion (LBPF) specimens, demonstrating its ability to handle size variability while maintaining precise and consistent quality control.

NOMENCLATURE

AM = Additive Manufacturing
CT = Computed Tomography
CAD = Computer-Aided Design
LBPF = Laser Powder Bed Fusion
XCT = X-ray Computed Tomography

1. Introduction

Metal AM has emerged as a viable alternative to traditional manufacturing methods for specific structural applications, offering notable advantages in design flexibility and material savings. To enhance the microstructure of Ti-6Al-4V titanium alloy, a 6-step optimized processing route was developed. This comprehensive process includes manufacturing, annealing, pressing, pre-matching, treatment, and final matching. The approach effectively reduces microvoid occurrence, thereby improving load-bearing performance and ensuring higher reliability in demanding applications [1]. By reducing microvoids to within 15 μm, the detrimental impact on fatigue performance is significantly minimized, resulting in a fatigue strength of approximately 1 GPa. In addition to the aforementioned process optimizations and hot isostatic pressing [2], various metal alloys are also being explored to further enhance the properties of metal AM components. A high-entropy alloy composed of CrMnFeCoNi was proposed in [3] to enhance damage tolerance and mechanical properties. This alloy's unique multi-element composition offers exceptional strength and ductility, making it a promising candidate for improving the performance of AM-manufactured components in demanding applications. By melting body-centered cubic structural Cr/Fe, face-centered cubic structural Ni, hexagonal close-packed Co, and complex A12 structural Mn, high-entropy alloys exhibit a remarkable strength-temperature relationship. These unique structural combinations enable superior mechanical performance across a range of temperatures. Such material and process innovations are pivotal in driving the expanding applications of metal AM, particularly in industries demanding high-performance and reliable components.

Energy-dispersive X-ray spectroscopy and X-ray diffraction are widely employed to analyze element distribution and microstructural characteristics. For instance, energy-dispersive X-ray spectroscopy has been used to characterize high-entropy alloys [4], while X-ray diffraction has been applied to investigate as-printed Ti–8.5Cu alloys [5]. Beyond these two techniques, X-ray is utilized on a larger scale for macro inspections and various applications [6]-[7]. XCT has proven effective in classifying internal AM defects such as lack of fusion, gas-entrapped pores, and keyholes [8], distinguishing it from fringe projection profilometry for external measurements [9]. To further enhance the XCT process and mitigate artifacts, CAD models and deep learning techniques have been integrated, significantly improving inspection speed and accuracy [10].

High-resolution XCT has proven effective in detecting and analyzing volumetric defects in metal AM. By extracting nine morphological parameters, three metal AM defects can be determined. However, despite its demonstrated capabilities, high-resolution XCT faces significant challenges that limit its broader application, including artifacts, slow scan speeds, and high costs. Moreover, the size of scanned metal AM specimens remains quite small, restricting its utility for large-scale components. For instance, the scanned region in [8] is a 1 mm × 1 mm × 1 mm cylinder, while the specimen in [10] is a 15 mm × 15 mm × 15 mm cylinder. While high-resolution XCT performs well in localized regions, its inability to provide global measurements is a critical limitation, particularly for large AM components. Currently, the scalability and measurement accuracy of XCT for metal AM remains underexplored, with no comprehensive reports addressing these issues in the community. This gap underscores the need for further advancements in XCT technology to support the characterization of larger-scale AM parts effectively.

To tackle this issue, this work proposes a scalable 3D XCT measurement strategy designed to deliver comprehensive global information for AM samples. The workflow for this approach is structured into seven key steps: grid location initialization, overlap optimization, linear blending fusion, projection size unification, 3D reconstruction, and volume analysis.

The structure of this work is organized as follows: Section 2 presents the scalable XCT measurement approach, including 2D projection stitching and the 3D scalable workflow. Section 3 describes the design of metal AM samples and experiments conducted for 3D assessment. Finally, Section 4 provides the conclusions.

2. Scalable 3D X-ray Computed Tomography Measurement Approach

To enable scalable measurements, the proposed strategy first stitches projection images in the 2D domain to encompass larger scanning regions, followed by 3D reconstruction to generate a complete volumetric model.

2.1 2D Projection Stitching Strategy

In the 2D domain, the proposed approach captures X-ray projection images while systematically adjusting the component's position within a predefined grid. This method ensures a consistent voxel size across all projections. Utilizing scanning location data directly from the XCT machine, the multi-scan locations are used to establish an initial grid framework for allocating the 2D projections accurately.

Starting from the initialized grid, the overlapping ratio is optimized to enhance the alignment of adjacent projections. A linear blending strategy is then employed to seamlessly manage overlapping areas between stitched images, ensuring expanded coverage of the metal AM component while preserving fine details. The complete 2D projection stitching strategy is illustrated in Fig. 1.

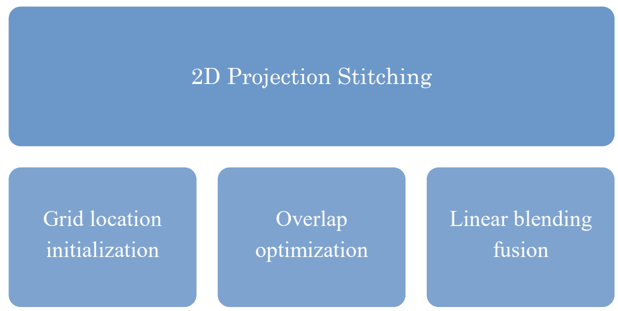

Fig. 1 2D projection stitching strategy.

2.2 3D Scalable Approach Workflow

Following the 2D projection stitching of individual projection images, all projection sizes are standardized to account for variations introduced by overlap optimization. With the unified 2D projection images, the filtered back projection algorithm [11] is utilized to reconstruct the 3D volume, producing the 3D volumetric data for the metal AM component. The entire workflow, from the 2D projection stitching strategy to the 3D scalable approach, is illustrated in Fig. 2.

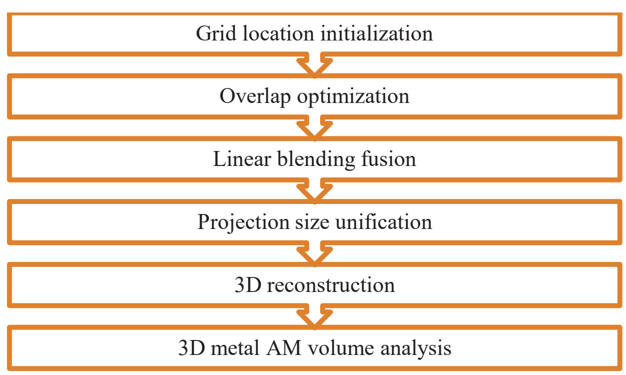

Fig. 2 3D scalable approach workflow.

3. Experiments and Accuracy Analysis

To validate the proposed strategy, a 105 mm test specimen made of

Inconel 718 is fabricated in accordance with the ASTM E466 standard practice [12], as shown in Fig. 3. Three complete XCT scans are performed at three different heights, spaced 5 mm apart. The corresponding 2D projection images captured at the same angle from each height are presented in Fig. 4.

Fig. 3 Metal AM test specimen.

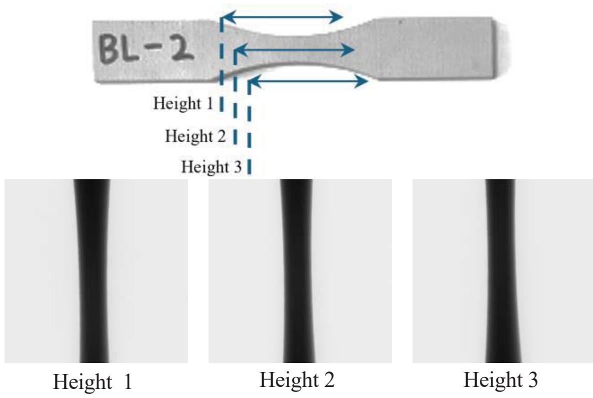

Fig. 4 2D projection images captured at different heights.

3.1 Scalability Performance in 2D

Through grid location initialization, overlap optimization, and linear blending fusion, the stitched 2D projection is visualized in Fig. 5. The original 2000 × 2000 image is extended to 2000 × 2638, showcasing the scalability of the proposed strategy.

Fig. 5 Scaled 2D projection images at a single scanning angle.

3.2 Scalability Performance in 3D

Using the stitched 2D projection image, 3D reconstruction is performed following the scalable approach workflow. The scalable result is visualized in Fig. 6(a). When compared to the center part without scaling in Fig. 6(b), the deviation range is [-0.3 mm, 0.3 mm], indicating good alignment. The top and bottom regions are both scaled using the Height 1 and Height 3 data.

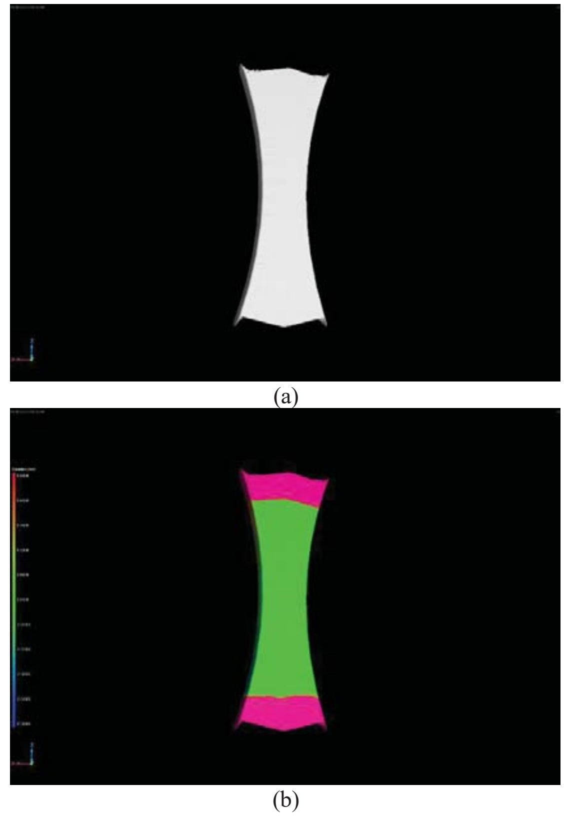

Fig. 6 Scaled 3D result and comparison.

3.3 Accuracy and Error Analysis

To further evaluate the scalability accuracy, two feature components are attached to the specimen for measurement. The component setup is shown in Fig. 7. The scaled result, with the extended portion highlighted in red, is presented in Fig. 8. The distance between the two cylinders is used to analyze the scalability accuracy, as shown in Table 1.

Fig. 7 Metal AM test specimen with feature components.

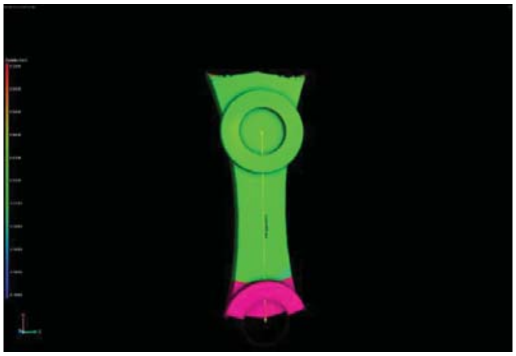

Fig. 8 Scaled 3D result and comparison.

Table 1 Accuracy assessment with feature components

Distance	Benchmark (mm)	XCT (mm)	Absolute Error (mm)	Relative Error (%)
Distance between two cylinder centers in Fig. 8	26.73 (Keyence Microsopy)	26.65 (XCT)	0.08	0.2
Nearest distance between two cylinders in Fig. 9	14.57 (Caliper)	15.00 (XCT)	0.43	2.9

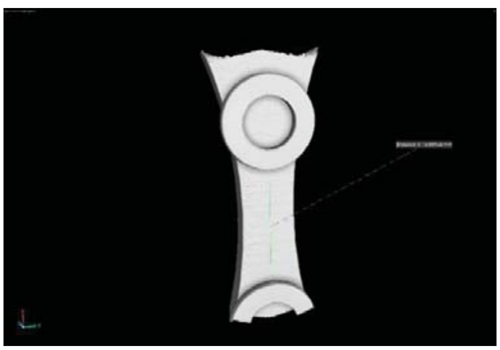

Fig. 9 Nearest distance between two cylinders.

4. Conclusions

To ensure the scanning resolution of large metal AM components, a scalable 3D XCT measurement approach is proposed, which involves stitching X-ray images in the 2D projection domain, followed by a reconstruction to generate the 3D volume.

The scalability performance is demonstrated both in 2D and 3D through the fabricated standard component. The external measurement error is within 2.9% when compared to microscopy and caliper measurements. While the proposed method is efficient, requiring only one reconstruction, further studies will explore comparisons with the direct 3D scaling approach.

ACKNOWLEDGEMENT

This research is supported by A*STAR under its RIE2025 Manufacturing, Trade and Connectivity (MTC) Industry Alignment Fund- Pre-Positioning (IAF-PP) (Award M24N2a0018).

REFERENCES

1. Qu, Z., Zhang, Z., Liu, R., Xu, L., Zhang, Y., Li, X., Zhao, Z., Duan, Q., Wang, S., Li, S. and Ma, Y., “High Fatigue Resistance in a Titanium Alloy via Near-void-free 3D Printing,” Nature, Vol. 626, No. 8001, pp. 999-1004, 2024.
2. Alegre, J.M., Díaz, A., García, R., Peral, L.B. and Cuesta, I.I., “Effect of HIP Post-processing at 850° C/200 MPa in the Fatigue Behavior of Ti-6Al-4V Alloy Fabricated by Selective Laser Melting,” International Journal of Fatigue, Vol. 163, pp.107097, 2022.
3. Gludovatz, B., Hohenwarter, A., Catoor, D., Chang, E.H., George, E.P. and Ritchie, R.O., “A Fracture-resistant High-entropy Alloy for Cryogenic Applications,” Science, Vol. 345, No. 6201, pp.1153-1158, 2014.
4. Ren, J., Zhang, Y., Zhao, D., Chen, Y., Guan, S., Liu, Y., Liu, L., Peng, S., Kong, F., Poplawsky, J.D. and Gao, G., “Strong Yet Ductile Nanolamellar High-entropy Alloys by Additive Manufacturing,” Nature, Vol. 608, No. 7921, pp.62-68, 2022.
5. Zhang, D., Qiu, D., Gibson, M.A., Zheng, Y., Fraser, H.L., StJohn, D.H. and Easton, M.A., “Additive Manufacturing of Ultrafine-Grained High-strength Titanium Alloys”. Nature, Vol. 576, No. 7785, pp.91-95, 2019.
6. Dong, C., Tan, A.W.W., Liu, T., Cheng, F. and Qian, K. “Transformer-based Smart Inspection for Agricultural Products via X-ray Images”. In International Conference on Optical and Photonic Engineering, Vol. 13069, pp.322-327, SPIE, 2024.
7. Dong, C., Liu, T., Cheng, F. and Qian, K. “X-ray Artificial Intelligence Identification System for Agricultural Products”, In Proc. of the 9th Intl. Conf. of Asian Society for Precision Engg. and Nanotechnology, 2022.
8. Poudel, A., Yasin, M.S., Ye, J., Liu, J., Vinel, A., Shao, S. and Shamsaei, N., “Feature-based Volumetric Defect Classification in Metal Additive Manufacturing,” Nature Communications, Vol. 13, No. 1, pp.6369, 2022.
9. Lv, S., Tang, D., Zhang, X., Yang, D., Deng, W. and Kemao, Q., “Fringe Projection Profilometry Method with High Efficiency, Precision, and Convenience: Theoretical Analysis and Development,” Optics Express, Vol. 30, No. 19, pp.33515-33537, 2022.
10. Ziabari, A., Venkatakrishnan, S.V., Snow, Z., Lisovich, A., Sprayberry, M., Brackman, P., Frederick, C., Bhattad, P., Graham, S., Bingham, P. and Dehoff, R., “Enabling Rapid X-ray CT Characterisation for Additive Manufacturing Using CAD Models and Deep Learning-based Reconstruction,” npj Computational Materials, Vol. 9, No. 1, pp.91, 2023.
11. Feldkamp L.A., Davis L.C. and Kress J.W., “Practical Cone-beam Algorithm,” Josa a, Vol. 1, No. 6, pp.612-619, 1984.
12. ASTM E466-21 Standard Practice for Conducting Force Controlled Constant Amplitude Axial Fatigue Tests of Metallic Materials. ASTM International, West Conshohocken, PA, ASTM, AI, 2021.